

On the Charge-Transfer Spectra of Iron(II)- and Ruthenium(II)-Tris(2,2'-bipyridyl) Complexes

A. Ceulemans and L. G. Vanquickenborne*

Contribution from the Department of Chemistry, University of Leuven, 3030 Heverlee, Belgium.
Received October 6, 1980

Abstract: Tris(2,2'-bipyridyl) complexes of divalent iron-group metals are characterized by a number of remarkable, low-lying charge-transfer states. A detailed elaboration of the intensity mechanism, governing these transitions, provides a direct understanding of an otherwise complex excited-state system. The treatment uses a general MO language and is mainly based on symmetry properties. As a result, new assignments are proposed for the visible and near-UV spectra of $M(\text{bpy})_3^{2+}$ complexes ($M = \text{Fe(II)}, \text{Ru(II)}$). Attention is drawn to the apparent spectroscopic relevance of the Orgel criterion for ligand orbital classification.

Introduction

The tris(2,2'-bipyridyl) complexes of iron(II), ruthenium(II), and also osmium(II) are of central importance in the study of energy- and charge-transfer processes.¹

Despite a considerable and widespread research interest, certain fundamental aspects of the electronic structure of the first excited states are not yet completely understood. The nature of the luminescent state of $\text{Ru}(\text{bpy})_3^{2+}$ is subject to continual debate;² the detailed assignment of the corresponding absorption bands in the visible region is equally difficult, although their metal-to-ligand charge-transfer (MLCT) character, described as $t_{2g} \rightarrow \pi^*$, has not been contested.

Following Orgel,³ any π or π^* ligand orbital can be classified with respect to a twofold rotation axis, bisecting the chelate angle; it is either symmetric, denoted χ , or antisymmetric, ψ . For our present purposes, we can represent them schematically as shown.



From a low-temperature spectroscopic investigation of oriented $M(\text{bpy})_3^{2+}$ complexes of the iron group ions in host crystals, Ferguson, Güdel, and co-workers⁴⁻⁶ concluded that both types of acceptor orbitals are involved in the visible charge-transfer absorptions. The charge-transfer configuration can therefore be described as $t_{2g} \rightarrow \pi^*(\psi)$, $\pi^*(\chi)$; we shall refer to this proposal as the $\psi+\chi$ hypothesis. The $\psi+\chi$ hypothesis is at variance with the current model of Hipps and Crosby,⁷ as well as with several semiempirical MO calculations⁸⁻¹⁰ available to date. Indeed all these previous studies concluded that only ψ -type acceptor orbitals can be excited in the visible region. The $t_{2g} \rightarrow \pi^*(\chi)$ transition was located at higher energy in the UV region.

The controversy finds its origin in the diverging points of view adopted by the two groups of authors: the ψ -only hypothesis is based on energy calculations, whereas the $\psi+\chi$ proposal is es-

entially based on an attempt to understand the intensity of the observed spectrum.

The latter method offers a valuable new perspective, if it can be reconciled with the constraints imposed by the orbital energy ordering. The dilemma—which apparently seems to exclude a reconciliation in the present case—can be solved if one uses an adequate model to calculate the distribution of intensity among the different dipole-allowed transitions in the tris-chelated complexes.

In what follows, we intend to describe a suitable coupled chromophore model, but first we shall present rather compelling evidence, from energy considerations, in favor of the ψ -only proposal.

Energy Characteristics

The energy gaps between ψ - and χ -type LUMO's in a series of α -diimine homologs were calculated by Nagakura et al.^{8,11,12} using a Pariser-Parr-Pople treatment and correcting for the presence of a coordinating metal center, in casu Fe(II). The energy gap was found to decrease with increasing number of π electrons, as could already be anticipated from Hückel calculations on the hydrocarbon analogs.¹³ In fact, three ligands were considered, in increasing order of complexity: α -diimine, with only four π electrons, 2,2'-bipyridyl, and 1,10-phenanthroline (phen).

In phenanthroline, which is the largest chelate of the series, the ψ and χ orbitals are calculated to be nearly degenerate.¹² In accordance with this result, the MLCT absorption of $M(\text{phen})_3^{2+}$ ($M = \text{Fe(II)}, \text{Ru(II)}$) provides a typical $\psi+\chi$ -like spectrum. It consists of a very broad band [$\Delta\nu_{1/2} \approx 0.6 \mu\text{m}^{-1}$], encompassing several transitions; the corresponding MCD spectrum can only be understood in a $\psi+\chi$ context.^{14,15}

On the other hand, in the simplest α -diimine chelate, with a butadiene-like π system, the χ orbital is calculated¹¹ at much higher energy than the ψ orbital ($\Delta E = 3.5 \text{ eV}$). Therefore, the first MLCT band is interpreted as being due to a typical ψ -only absorption. Illustrative examples can be found in the visible spectra^{9,16} of $\text{Fe}(\text{gmi})_3^{2+}$ and of $\text{Ru}(\text{bt})_3^{2+}$. Indeed, both gmi and bt ligands¹⁷ have an olefinic structure, which is identical with α -diimine. The spectra consist of one isolated absorption region having a bandwidth which is only half that of the phen complexes, and characterized by a typical doublet appearance.

(1) V. Balzani, F. Bolletta, M. T. Gandolfi, and M. Maestri, *Top. Curr. Chem.*, **75**, 1 (1978).

(2) K. W. Hipps, *Inorg. Chem.*, **19**, 1390 (1980).

(3) L. E. Orgel, *J. Chem. Soc.*, 3683 (1961).

(4) F. Felix, J. Ferguson, H. U. Güdel, and A. Ludi, *Chem. Phys. Lett.*, **62**, 153 (1979).

(5) F. Felix, J. Ferguson, H. U. Güdel, and A. Ludi, *J. Am. Chem. Soc.*, **102**, 4096 (1980).

(6) S. Decurtins, F. Felix, J. Ferguson, H. U. Güdel, and A. Ludi, *J. Am. Chem. Soc.*, **102**, 4102 (1980).

(7) K. W. Hipps and G. A. Crosby, *J. Am. Chem. Soc.*, **97**, 7042 (1975).

(8) I. Hanazaki and S. Nagakura, *Inorg. Chem.*, **8**, 649 (1969).

(9) J. Blomquist, B. Nordén, and M. Sundbom, *Theor. Chim. Acta*, **28**, 313 (1973).

(10) B. Mayoh and P. Day, *Theor. Chim. Acta*, **49**, 259 (1978).

(11) T. Ito, N. Tanaka, I. Hanazaki, and S. Nagakura, *Bull. Chem. Soc. Jap.*, **41**, 365 (1968).

(12) T. Ito, N. Tanaka, I. Hanazaki, and S. Nagakura, *Bull. Chem. Soc. Jap.*, **42**, 702 (1969).

(13) C. A. Coulson and A. Streitwieser, Jr., "Dictionary of π -Electron Calculations", Pergamon Press, Oxford-Frankfurt, 1965.

(14) B. R. Hollebone, S. F. Mason, and A. J. Thomson, *Symp. Faraday Soc.*, **3**, 146, 159 (1969).

(15) A. J. McCaffery, S. F. Mason, and B. J. Norman, *J. Chem. Soc. A*, 1428 (1969).

(16) W. P. Krug and J. N. Demas, *J. Am. Chem. Soc.*, **101**, 4394 (1979).

(17) gmi: glyoxal bis-*N*-methylimine; bt: 2,2'-bi-2-thiazoline.

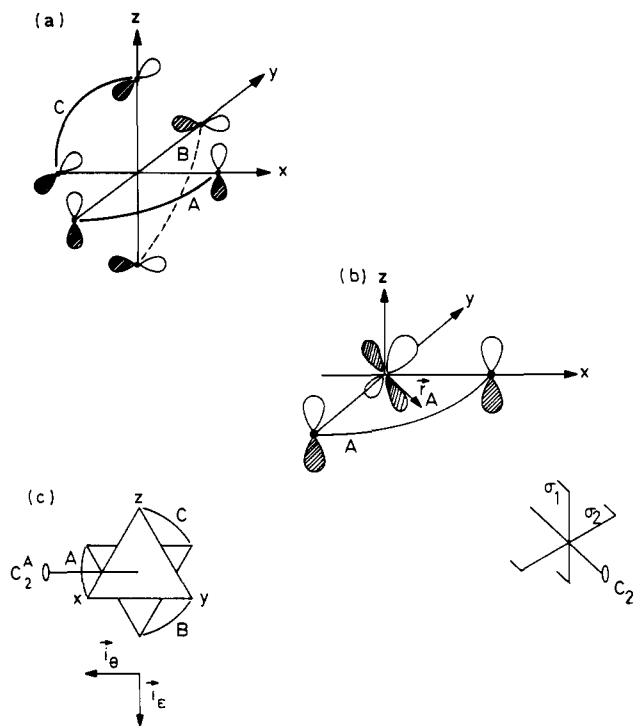


Figure 1. (a) Standard coordinate choice for D_3 complex. ψ -type ligand orbitals are shown schematically. (b) Detailed view of the monochromophore with ligand A. The figure shows the $b_1^0(t_{2g})$ donor orbital and the $b_1^0(\psi)$ acceptor orbital, as well as the C_{2v} -group elements. (c) Trigonal projection of a tris-chelated complex and orthonormal directions of σ polarization.

Precisely these same qualitative features^{5,6} arise in the visible spectra of $Fe(bpy)_3^{2+}$ and $Ru(bpy)_3^{2+}$, providing phenomenological evidence for a ψ -only LUMO. Moreover, in the solution spectrum of $Fe(bpy)_3^{2+}$ the second MLCT absorption is found at $\sim 0.9 \mu m^{-1}$ above the first one. This is in good agreement with the MO studies,⁸ the $t_{2g} \rightarrow \pi^*(\chi)$ transition is calculated at $\sim 1.2 \mu m^{-1}$ above the $t_{2g} \rightarrow \pi^*(\psi)$ transition.

In the ruthenium(II) analogue, the $t_{2g} \rightarrow \pi^*(\chi)$ absorption is masked by intense intraligand transitions. However, in a series of substituted complexes such as $cis-M(bpy)_2X_2$,¹⁸⁻²¹ where X is a σ or π -donor ligand, the optical electronegativity of the metal t_{2g} -donor orbitals can be markedly decreased; a consequent overall red shift of the entire MLCT absorption system is observed, while the intraligand absorptions remain virtually unaltered. As a result, in these cis -disubstituted complexes, both transitions $t_{2g} \rightarrow \pi^*(\psi)$ and $t_{2g} \rightarrow \pi^*(\chi)$ can be identified separately. They are situated at a constant interval of each other, irrespective of nature of X. In the iron(II) case, this interval is about $0.9 \mu m^{-1}$, exactly as in $Fe(bpy)_3^{2+}$. For $cis-Ru(bpy)_2X_2$ a constant interval of $0.75 \mu m^{-1}$ is observed.¹⁸

As a conclusion, Nagakura's calculations appear to be supported by rather strong experimental evidence. The ψ -only nature of the first MLCT absorption region for the bpy complexes can be considered quite well established. Yet, according to Ferguson and Güdel,⁴⁻⁶ this ψ -only configuration manifold cannot account for the typical doublet structure of the visible $M(bpy)_3^{2+}$ spectra. Therefore, our principal concern is a reassessment of the intensity calculation, on which these conclusions were based.

The Theoretical Model

A. Monochelated Complexes. The origin of the intensity in a hypothetical monochelated entity has been discussed by Day

and Sanders,²² following earlier treatments by Mulliken²³ and Murrell.²⁴ The monochromophore has C_{2v} symmetry. From the outset, we will use the standard coordinate system³ for the trischelated complex (Figure 1a). At first only one ligand, say A, is considered. The C_{2v} -symmetry elements are defined in Figure 1b. The ψ -type orbital on the ligand, ψ_A , transforms as b_1 . Within the t_{2g} subshell only one symmetry-adapted linear combination (SALC) with the same symmetry characteristics is available. We shall denote it in zeroth order as:

$$b_1^0(t_{2g}) = \frac{1}{\sqrt{2}}(d_{xz} - d_{yz}) \quad (1)$$

Its phase is defined so as to obtain a positive overlap with ψ_A , as indicated in Figure 1b. In what follows, the superscript will be used to denote zeroth-order orbitals; in first-order, the zero is dropped.²⁵ To fall in line with this notation, we will also use $\psi_A = b_1^0(\psi)$.

The two b_1 orbitals can interact with each other, resulting in a bonding combination, mainly localized on the metal donor, denoted $b_1(t_{2g})$, and an antibonding combination, $b_1(\psi)$, mainly localized on the ligand acceptor. Using first-order perturbation theory, one finds:²²

$$b_1(t_{2g}) = b_1^0(t_{2g}) + cb_1^0(\psi) \quad b_1(\psi) = b_1^0(\psi) - cb_1^0(t_{2g}) \quad (2)$$

where c is the first-order mixing coefficient.²⁶

From group theoretical considerations, it is obvious that the $b_1(t_{2g}) \rightarrow b_1(\psi)$ transition has to be polarized along the C_2 axis, that is, in the direction of the charge transfer. Let us denote a vector in this direction as r_A , centered on the metal and directed toward the center of the A ligand. As discussed by Day and Sanders,²² the main contribution to the intensity comes from the so-called transfer term, which is the one-center term on the ligand:

$$\langle b_1(t_{2g}) | q r_A | b_1(\psi) \rangle = c \langle \psi_A | q r_A | \psi_A \rangle = c q R \quad (3)$$

R is the position vector of the ligand center, and q the electronic charge.

In this simple case of one acceptor ligand, the diagonal matrix element in eq 3, qR , is a measure for the dipole moment of the transferred charge.²² Since the transfer term for the monochelated complex is a basic quantity of the model, we define a new parameter κ :

$$\kappa = c q |R| \quad (4)$$

Evidently, any metal orbital that does not overlap with the ligand functions cannot give rise to ligand-centered integrals of the type discussed in eq 3; therefore, the corresponding transitions are deprived of any intensity from transfer terms.²³

Basically the same conclusion holds true for the tris-chelated complexes, where the presence of three acceptor sites is responsible for a total $t_{2g} \rightarrow \pi^*$ transition probability, which will be three times that of a monocomplex.²² On the other hand, in this case the dipole moment of the transferred charge will be exactly zero by symmetry.

In order to relate the dipole strength in the tris complexes to the quantity κ , we will develop a more detailed model of three coupled chromophores; we will do so within the framework of an approximate MO formalism. A somewhat similar procedure has been used before in the description of LMCT spectra of ruthenium(III)- and osmium(III)-halogeno ammine complexes.²⁷

B. Trischelated Chromophores. The $M(bpy)_3^{2+}$ moiety has exact D_3 symmetry²⁸ (Figure 1a,c). In this group the metal t_{2g}

(18) G. M. Bryant, J. E. Fergusson, and H. K. J. Powell, *Aust. J. Chem.*, **24**, 257 (1971).

(19) B. Durham, J. L. Walsh, C. L. Carter, and T. J. Meyer, *Inorg. Chem.*, **19**, 860 (1980).

(20) G. M. Brown, T. R. Weaver, F. R. Keene, and T. J. Meyer, *Inorg. Chem.*, **15**, 190 (1976).

(21) D. M. Klassen and G. A. Crosby, *J. Chem. Phys.*, **48**, 1853 (1968).

(22) P. Day and N. Sanders, *J. Chem. Soc. A*, 1536 (1967).

(23) R. S. Mulliken, *J. Am. Chem. Soc.*, **74**, 811 (1952).

(24) J. N. Murrell, "The Theory of the Electronic Spectra of Organic Molecules", Methuen, London, 1963, Chapter 7.

(25) The SALC matching χ_A corresponds to $a_2^0(t_{2g}) = (1/\sqrt{2})(d_{xz} + d_{yz})$.

(26) Because of the here adopted phase convention, c is positive.

(27) E. Verdonck and L. G. Vanquickenborne, *Inorg. Chem.*, **13**, 762 (1974).

(28) D. P. Rillema, D. S. Jones, and H. A. Levy, *J. Chem. Soc., Chem. Commun.*, 849 (1979).

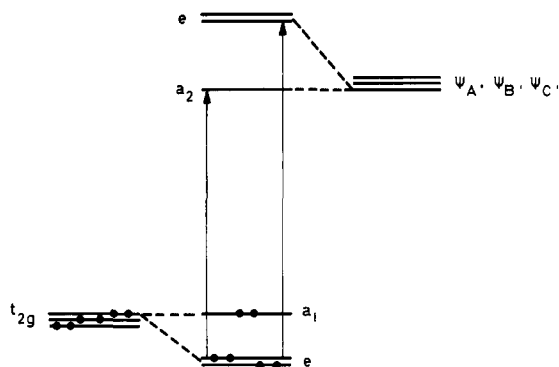


Figure 2. Orbital interaction diagram of metal t_{2g} - and ligand ψ -type orbitals. The two allowed D_3 transitions are indicated. See also ref 7.

Table I. Symmetry Properties of e_θ and e_ϵ Functions^a

	C_3	C_2^A
e_θ	$-(1/2)e_\theta + (\sqrt{3}/2)e_\epsilon$	e_θ
e_ϵ	$-(\sqrt{3}/2)e_\theta - (1/2)e_\epsilon$	$-e_\epsilon$

^a See ref 29, Tables A16 and A17.

orbitals transform as a_1 and e . The three ligand orbitals (ψ_A , ψ_B , ψ_C) span a basis for an a_2 and e representation. Since only the e -type orbitals can interact, one expects an orbital ordering as shown in Figure 2. Clearly many excited states result from the $(t_{2g})^5(\pi^*(\psi))^1$ charge-transfer configuration. A description of this manifold can profitably make use of symmetry, if the proper conventions are made in defining the components of the degenerate e representation. Following Griffith, the two components are chosen to be qualified with respect to the C_2 axis, bisecting the A ligand.²⁹ We introduce e_θ and e_ϵ to describe the symmetry behavior as expressed in Table I.³⁰ From the table, it is evident that the phase choice for any e_θ function determines the phase of the corresponding e_ϵ function.

(i) **Basis Functions.** Table II lists the symmetry-adapted, zeroth-order metal and ligand orbitals. Also χ -type acceptor orbitals are included. Orbital phases are chosen so that all nonzero metal-ligand overlap integrals are positive. Only functions with the same symmetry labels can interact with each other. To first order in perturbation theory, one obtains the bonding and antibonding combinations in the same way as in eq 2:

$$\begin{aligned} e_\epsilon(t_{2g}) &= e_\epsilon^0(t_{2g}) + c(e; t_{2g}, \psi) \cdot e_\epsilon^0(\psi) \\ e_\epsilon(\psi) &= e_\epsilon^0(\psi) - c(e; t_{2g}, \psi) \cdot e_\epsilon^0(t_{2g}) \end{aligned} \quad (5)$$

The D_3 mixing coefficient of eq 5 can be related to the coefficient c for the monochelated case (eq 2), by evaluating the appropriate resonance integral. We find:

$$c(e; t_{2g}, \psi) = \sqrt{\frac{3}{2}} c \quad (6)$$

Let c' be the counterpart of c for a χ -type monochelated complex. From Table II, it is clear that in a D_3 complex with χ -acceptor orbitals both $a_1^0(t_{2g})$ and $e^0(t_{2g})$ orbitals can mix with ligand functions. One has

$$c(a_1; t_{2g}, \chi) = \sqrt{2}c \quad c(e; t_{2g}, \chi) = \frac{1}{\sqrt{2}}c \quad (7)$$

The excitations of the monocomplexes are polarized along the individual C_2 axes; therefore, they cannot provide intensity parallel to the C_3 axis.²² This is consistent with the dominant σ -polarized ($\perp C_3$) spectrum, observed in the tris complex.³¹ Now, let i_A ,

Table II. Symmetry Adapted Zeroth-Order Orbital Functions for Metal t_{2g} Orbitals and Ligand ψ - and χ -Type Acceptor Orbitals

t_{2g} orbitals
$a_1^0(t_{2g}) = \frac{1}{\sqrt{3}}(d_{xy} + d_{xz} + d_{yz})$
$e_\theta^0(t_{2g}) = \frac{1}{\sqrt{6}}(-2d_{xy} + d_{yz} + d_{xz})$
$e_\epsilon^0(t_{2g}) = \frac{1}{\sqrt{2}}(d_{xz} - d_{yz})$
ψ orbitals
$a_2^0(\psi) = \frac{1}{\sqrt{3}}(\psi_A + \psi_B + \psi_C)$
$e_\theta^0(\psi) = \frac{1}{\sqrt{2}}(\psi_C - \psi_B)$
$e_\epsilon^0(\psi) = \frac{1}{\sqrt{6}}(2\psi_A - \psi_B - \psi_C)$
χ orbitals
$a_1^0(\chi) = \frac{1}{\sqrt{3}}(\chi_A + \chi_B + \chi_C)$
$e_\theta^0(\chi) = \frac{1}{\sqrt{6}}(2\chi_A - \chi_B - \chi_C)$
$e_\epsilon^0(\chi) = \frac{1}{\sqrt{2}}(\chi_B - \chi_C)$

i_B , and i_C be the unit vectors in the directions of the respective ligand centers. The σ -directed unit vectors, transforming as e_ϵ and e_θ , can be written:

$$i_\theta = i_A \quad i_\epsilon = \frac{1}{\sqrt{3}}(i_B - i_C) \quad (8)$$

From Figure 1c, it is obvious that i_A , i_B , and i_C are nonorthogonal:

$$i_A \cdot i_B = i_B \cdot i_C = i_C \cdot i_A = -1/2 \quad (9)$$

qr_θ and qr_ϵ are the dipole operator components in the so-defined σ directions.

(ii) **Orbital Transition Moments.** Using the basis functions of Table II, and their first-order corrections (eq 6 and 7), one can now calculate the contribution of the transfer term in the different orbital transitions. First consider the excitations $t_{2g} \rightarrow \pi^*(\psi)$ (Figure 2). In principle, three σ -polarized orbital transitions can occur: $a_1 \rightarrow e$, $e \rightarrow a_2$, and $e \rightarrow e$.

Since the $a_1^0(t_{2g})$ orbital is not affected by interactions with the ligand orbitals, the corresponding $a_1 \rightarrow e$ transition cannot carry intensity from a transfer term; this parallels the conclusions of the preceding section.

Next consider the transition $e(t_{2g}) \rightarrow a_2(\psi)$. Although these orbitals do not overlap with each other, they do give rise to a ligand centered integral, since the $e(t_{2g})$ orbital is partially delocalized over the ligands, by virtue of the $e^0(\psi) - e^0(t_{2g})$ interaction. From eq 5 and 6, the transfer contribution to the symmetry-allowed dipole moment, e.g., the θ component, can easily be derived:

$$\langle e_\epsilon(t_{2g}) | qr_\theta | a_2(\psi) \rangle = \sqrt{\frac{3}{2}} c \langle e_\epsilon^0(\psi) | qr_\theta | a_2^0(\psi) \rangle \quad (10)$$

We will adopt a weak coupling between the ligands, so that the interligand interactions can be supposed to be much less important than the intraligand contributions. If so, the ligand-centered matrix element in eq 10 can be approximated as:

$$\langle e_\epsilon^0(\psi) | qr_\theta | a_2^0(\psi) \rangle = \frac{1}{3\sqrt{2}} (2\langle \psi_A | qr_A | \psi_A \rangle - \langle \psi_B | qr_A | \psi_B \rangle - \langle \psi_C | qr_A | \psi_C \rangle) \quad (11)$$

In eq 11 $\langle \psi_B | qr_A | \psi_B \rangle$ is the projection of the dipole moment

(29) J. S. Griffith, "The Theory of Transition-Metal Ions", Cambridge University Press, London, 1971.

(30) Usually these symbols refer to O_h symmetry. Their meaning is, however, also in agreement with Table I in the D_3 subgroup (see also ref 28, Table A17).

Table III. D₃ Orbital Transition Moments

$q\tau\theta$	$ a_2(\psi)\rangle$	$ e_\theta(\psi)\rangle$	$ e_e(\psi)\rangle$	$ a_1(\chi)\rangle$	$ e_\theta(\chi)\rangle$	$ e_e(\chi)\rangle$
$\langle a_1(t_{2g}) $	\cdot	\cdot	\cdot	\cdot	\cdot	\cdot
$\langle e_\theta(t_{2g}) $	\cdot	$-(\sqrt{3/8})\kappa$	\cdot	$(1/2)\kappa'$	$(1/\sqrt{8})\kappa'$	\cdot
$\langle e_e(t_{2g}) $	$(\sqrt{3/2})\kappa$	\cdot	$(\sqrt{3/8})\kappa$	\cdot	\cdot	$-(1/\sqrt{8})\kappa'$
$q\tau_e$						
$\langle a_1(t_{2g}) $	\cdot	\cdot	\cdot	\cdot	\cdot	\cdot
$\langle e_\theta(t_{2g}) $	$-(\sqrt{3/2})\kappa$	\cdot	$(\sqrt{3/8})\kappa$	$(1/2)\kappa'$	$-(1/\sqrt{8})\kappa'$	$-(1/\sqrt{8})\kappa'$
$\langle e_e(t_{2g}) $	\cdot	$(\sqrt{3/8})\kappa$	\cdot	\cdot	\cdot	\cdot

^a κ and κ' represent the elementary moments in a monochelated complex with respectively ψ - and χ -type acceptor orbitals (eq 4). All matrix elements should be multiplied by the unit vectors i_θ and i_e , respectively.

Table IV. Summary of State Transition Moments for the Different ¹A₁ → ¹E Excitations

orbital transition	transition moment	
	ψ acceptor	χ acceptor
¹ E($a_1 \rightarrow e$)	0	$\sqrt{2}\kappa'$
¹ E($e \rightarrow a_2, a_1$)	$(\sqrt{3/2})\kappa$	$(1/\sqrt{2})\kappa'$
¹ E($e \rightarrow e$)	$(\sqrt{3/2})\kappa$	$(1/\sqrt{2})\kappa'$

$\langle \psi_B | q\tau_B | \psi_B \rangle$ in the i_A direction. It can be related to the corresponding quantity for the A ligand, by

$$\langle \psi_B | q\tau_B | \psi_B \rangle = (i_A \cdot i_B) \langle \psi_A | q\tau_A | \psi_A \rangle \quad (12)$$

Combining these equations with eq 9, one has finally:

$$\langle e_e(t_{2g}) | q\tau_\theta | a_2(\psi) \rangle = \frac{1}{2\sqrt{3}} (2 - i_A \cdot i_B - i_C \cdot i_A) \kappa i_\theta = \frac{\sqrt{3}}{2} \kappa i_\theta \quad (13)$$

In the same way, all other orbital transition moments equally appear as the product of a symmetry-determined coupling coefficient³² and one single parameter κ . Table III summarizes these results.

(iii) **State Transition Moments.** The final step in our model analyzes transition integrals over state functions into elementary orbital transitions. The relevant state functions can be obtained using standard procedures. The ground state is a totally symmetric singlet ¹A₁ characterized by the closed-shell configuration: $(a_1 - (t_{2g})^2)(e(t_{2g}))^4$, or $|a_1 \bar{a}_1 \bar{\theta} \bar{\theta} \bar{e} \bar{e}\rangle$ for short.

To each orbital transition, considered in the previous section, one σ -polarized ¹A₁ → ¹E transition can be associated. As an example, consider the wave functions of ¹E($e \rightarrow a_2$):

$${}^1E_\theta(e \rightarrow a_2) = (1/\sqrt{2})(|a_1 \bar{a}_1 \bar{\theta} \bar{e} \bar{a}_2\rangle - |a_1 \bar{a}_1 \bar{\theta} \bar{e} \bar{a}_2\rangle) \quad (14)$$

$${}^1E_e(e \rightarrow a_2) = -(1/\sqrt{2})(|a_1 \bar{a}_1 \bar{\theta} \bar{e} \bar{a}_2\rangle - |a_1 \bar{a}_1 \bar{\theta} \bar{e} \bar{a}_2\rangle)$$

The symmetry properties of these determinantal wave functions³³ obey Table I; their phases are therefore interrelated. The transition moments can be found quite readily with the aid of Table III.

$$\langle {}^1A_1 | q\tau_\theta | {}^1E_\theta(e \rightarrow a_2) \rangle = \sqrt{2} \langle e_e(t_{2g}) | q\tau_\theta | a_2(\psi) \rangle = (\sqrt{3/2}) \kappa i_\theta$$

$$\langle {}^1A_1 | q\tau_e | {}^1E_e(e \rightarrow a_2) \rangle = -\sqrt{2} \langle e_\theta(t_{2g}) | q\tau_e | a_2(\psi) \rangle = (\sqrt{3/2}) \kappa i_e \quad (15)$$

Similarly, for the $e \rightarrow e$ transition:

$$\langle {}^1A_1 | q\tau_\theta | {}^1E_\theta(e \rightarrow e) \rangle = \langle e_e(t_{2g}) | q\tau_\theta | e_e(\psi) \rangle - \langle e_\theta(t_{2g}) | q\tau_\theta | e_\theta(\psi) \rangle = (\sqrt{3/2}) \kappa i_\theta$$

$$\langle {}^1A_1 | q\tau_e | {}^1E_e(e \rightarrow e) \rangle = \langle e_\theta(t_{2g}) | q\tau_e | e_e(\psi) \rangle + \langle e_e(t_{2g}) | q\tau_e | e_\theta(\psi) \rangle = (\sqrt{3/2}) \kappa i_e \quad (16)$$

(32) Reference 28, Table A20.

(33) L. G. Vanquickenborne and A. Ceulemans, *Chem. Phys. Lett.*, **75**, 494 (1980).

Table V. New Assignments for the MLCT Spectra of Fe(bpy)₃²⁺ and Ru(bpy)₃²⁺^a

assignment	Fe(II)	Ru(II)
¹ E($e \rightarrow a_2(\psi)$)	1.862	2.155
¹ E($e \rightarrow e(\psi)$)	2.028	2.336
¹ E($a_1 \rightarrow e(\chi)$)	2.861 ^b	(2.960) ^c

^a Visible spectra were measured in Zn(bpy)₃(SO₄)·7H₂O at 8 K (from ref 5 and 6). ^b Observed in methanol solution; see ref 18. ^c Masked by ligand-centered transitions; see text.

A summary of all relevant state transition moments is presented in Table IV. From this table, we predict that the $t_{2g} \rightarrow \pi^*(\psi)$ excitation in a tris-chelated complex will be characterized by two major absorption bands of roughly equal intensity. If instead a χ -type acceptor orbital is involved, one intense peak is expected, with two minor satellites, with relative intensity magnitude as 4:1:1. Moreover, if interligand interactions are small, the total dipole strength equals three times that for a monochelated complex.³⁴

Conclusion and Comparison with Experiment

Ferguson et al.⁴ have argued that the two prominent peaks in the visible MLCT spectrum cannot be attributed to the vibrational structure of one single electronic transition, but instead must be assigned to two different excited states. While we concede their argument, Table IV suggests that this doublet structure can immediately be related to the two intense absorptions: ¹E($e \rightarrow a_2$) and ¹E($e \rightarrow e$), indicated in Figure 2. There is no need to invoke a $\psi + \chi$ hypothesis, which seems incompatible with energy considerations.

Using the orbital order in Figure 2, we propose specific assignments for the visible and the near-UV absorption spectra in Table V.

At first sight, the spectrum of Os(bpy)₃²⁺ is considerably more complex than the iron and ruthenium analogues⁵ and is, therefore, not included in Table V. Several factors might intervene in this case, e.g., the much larger spin-orbit coupling⁵ or significant delocalization of metal orbitals toward the ligands. Similar effects are known to occur in osmium porphyrins.³⁵ It can be expected that more fine-structure information will become available from CD and MCD studies, and from substituted chelate complexes.³⁶

Acknowledgment. Financial support by the Belgian Government (Programmatie van het Wetenschapsbeleid) is gratefully acknowledged. One of us (A.C.) is indebted to the "Nationaal Fonds voor Wetenschappelijk Onderzoek" for a research grant.

(34) The dipole strength for a monochelated complex is given by $2\kappa^2$ or $2\kappa'^2$.

(35) J. W. Büchler, W. Kokish, and P. D. Smith, *Struct. Bonding (Berlin)*, **34**, 79–134 (1978).

(36) J. Ferguson, A. W. H. Mau, and W. H. Sasse, *Chem. Phys. Lett.*, **68**, 21 (1979).